RSC Advances

PAPER

View Article Online
View Journal | View Issue

Cite this: *RSC Adv.*, 2020, **10**, 43523

Preparation of antistatic epoxy resin coatings based on double comb-like quaternary ammonium salt polymers

Wei Gao,[a] Zeng-chao Dang,[a] Fu-sheng Liu, *[a] Sheng Wang,*[b] Duan-wei Zhang[a] and Meng-xi Yan[b]

Received 31st August 2020
Accepted 25th November 2020

DOI: 10.1039/d0ra07479a

rsc.li/rsc-advances

Two kinds of double comb-like quaternary ammonium salt polymers P(DPA-EPI) and P(DBA-EPI) with lower polarity were designed and synthesized using epichlorohydrin (EPI), di-*n*-propylamine (DPA) and di-*n*-butylamine (DBA) as raw materials. The transparent antistatic epoxy resin coatings were obtained using the two polymers as antistatic agents, respectively. Because P(DPA-EPI) and P(DBA-EPI) with good hygroscopic performance are easily dissolved in epoxy resin paints and are nearly linearly arranged in the epoxy resin paints, the obtained transparent antistatic epoxy resin coatings achieve good antistatic properties. The values of ρ_s of the coatings reach $5.13 \times 10^8\ \Omega\ sq^{-1}$ and $2.69 \times 10^8\ \Omega\ sq^{-1}$, respectively, with a lower addition amount of polymers of only 1.0 wt%. The two antistatic epoxy resin coatings also have good durability. Compared to the epoxy resin coating, with the introduction of P(DPA-EPI) and P(DBA-EPI), the thermal stability and adhesion of the antistatic epoxy resin coatings do not change obviously, but the Rockwell hardness values slightly reduce.

1. Introduction

Epoxy resin coating has the advantages of strong adhesion, high strength, good heat resistance, good oil and alkali resistance and high toughness. It is widely used in many fields covering coatings for large storage tanks, pipelines and chemical equipment, *etc.* However, epoxy resin is generally low in moisture absorption and high in electric insulation. Therefore, epoxy resin is easily charged by static electricity. The accumulated electrostatic charges may generate discharges and even create the danger of explosions.[1,2] The way of incorporating an antistatic agent into the epoxy resin coating to increase its antistatic ability is the most effective way to solve the problem of electrostatic hazards of coatings.

Antistatic agents used in coatings mainly include surfactants, conductive fillers and polymer antistatic agents. As antistatic agent, the surfactant has a relatively small molecular weight with the hydrophilic groups incompatible with the resin and the lipophilic groups such as oily long-chain hydrocarbon groups compatible with the resin.[3,4] After the surfactant is mixed with the epoxy resin paint, the surfactant molecules form the orientation arrangement at the interface between the paint and the air, in which the lipophilic groups extend to the inside of the resin and the hydrophilic groups extend to the outside of the resin. After the epoxy resin paint is cured to form epoxy resin coating, the hydrophilic groups arranged on the side toward the air absorb environmental moisture to form a conductive water film, which reduces the value of surface resistivity of the coating to achieve the purpose of releasing static electricity. However, the surfactant does not produce a durable effect because the antistatic layer on the surface of the coating can easily be removed by friction, touching and washing in the course of using resulting the reducing of the antistatic performance. Although after a period of time, the surfactant molecules inside the coating will migrate to the surface to restore the antistatic performance, but long-term friction and contact will cause the antistatic performance continuously to decrease and eventually disappear. Therefore, the surfactant with a relatively small molecular weight cannot endow the resin with a persistently antistatic ability, due to its deterioration of antistatic performance with time. The surfactant can be divided into cationic surfactant, anionic surfactant, nonionic surfactant and zwitterionic surfactant according to the chemical structure. Among them, quaternary ammonium salt, a cationic surfactant, is widely used as a conventional antistatic agent because the good antistatic property.[5,6]

Conductive fillers are the powder materials with conductive properties. There are many types of conductive fillers, including polypyrroles,[7] polyanilines,[8] graphene,[9] carbon nanotube,[10,11] carbon fiber[12] silver powder,[13] copper powder[14] and nickel powder,[15] *etc.* When the conductive fillers are used as the antistatic agents, the powders form a conductive network structure

[a]*Department of Chemistry and Materials Science, College of Science, Nanjing Forestry University, Nanjing 210037, P. R. China. E-mail: lfs039270@163.com; l_iufusheng62@163.com*

[b]*College of Chemical Engineering, Nanjing Tech University, Nanjing 210009, P. R. China. E-mail: W_angsheng@njtech.edu.cn*

in the coating to achieve the purpose of releasing static electricity.[16] Compared with surfactants, the conductive fillers are long-lasting and stable because the antistatic effects will not be lost during the process of friction and touching.[14] However, sufficient antistatic effects of conductive fillers are achieved only when the concentration of conductive fillers exceeds a percolation threshold, which is generally at around or more than several percent.[17,18] The addition amount of conductive fillers are related to many factors, such as the particle size, conductivity and dispersion of the conductive fillers.[12] Increasing the amount of conductive fillers adding into the epoxy resin coatings can form a more complete conductive network structure, which is beneficial to dissipate the static, but it will also have a significant impact on the mechanical and physical properties of the epoxy resin coatings. In addition, in order to make the conductive fillers evenly distribute in the epoxy resin coatings, it is necessary to increase the processes such as pre-mixing and three-roll grinding,[11] which increases the using cost by increasing the complexity.

Polymer antistatic agents are generally polymers with a certain polarity. After being mixed with the resins, they are distributed in the resins to form a structure of microphase separation liking the shape of fine ribs or islands.[19] When the addition amount of polymer antistatic agents reaches or exceeds the threshold value, a conductive network channel is formed resulting effectively releasing static electricity by adsorbing environmental moisture to form a conductive water film. Bao *et al.*[20] have successfully prepared an antistatic poly(-vinyl chloride)/quaternary ammonium salt based ion-conductive acrylate copolymer (PVC/QASI) in a Haake torque rheometer. The surface resistivity of the PVC/QASI composites could be reduced to 10^7 Ω sq^{-1} order of magnitude when the QASI content reached 20 phr (parts per hundreds of resin). Tsurumaki *et al.*[18] also reported that the surface and volume resistivities are hundred times smaller than those of pristine polyether-based polyurethane (PU) by using ionic liquid (IL) fillers, which are composed of polymerized [2-(methacryloyloxy) ethyl]trimethylammonium bis(trifluoromethanesulfonyl)imide as antistatic agents. The antistatic property of the polymer antistatic agent is long-lasting and stable,[19] but it also suffers the problem of larger addition amount required to meet the antistatic requirements resulting the changing of the mechanical and physical properties of the resins. Therefore, the preparation of a polymer antistatic agent with persistently antistatic ability and good compatibility in the resin, which can remove static electricity by adding a smaller amount and make less changes in the mechanical and physical properties of the resin, has attracted much more attention.

The quaternary ammonium salt polymer, a polymer antistatic agent, is a type of polymer containing quaternary ammonium salt groups linked on the branch[20] or on the main chain, such as epichlorohydrin–dimethylamine copolymer,[21] epichlorohydrin–diethylamine copolymer,[22] epichlorohydrin–diethanolamine copolymer,[23] poly dimethyl diallyl ammonium chloride[24] and so on. But the above quaternary ammonium salt polymers have good solubility in water, but insolubility in epoxy resin paints. So they should not be used as antistatic agents for the epoxy resin coating, but as flocculants for water treatment. The solubility of quaternary ammonium salt polymers is related to the structure of the main chain and the branch. Generally, the lower mass ratio of quaternary ammonium salt groups in the polymer molecule has the better oil solubility. Thus, the oil solubility of the quaternary ammonium salt polymers can be adjusted by changing the proportion of the quaternary ammonium salt groups in the molecule, as a result, it can be dissolved in the epoxy resin.

Comb-like polymer is a kind of polymer with special structure composed of the polymer main chain and the pendent side chains. Both the structural compositions of the main chain and the polarity and length of the side chain play an important role in its structure and performance. The synergistic effect of the main chain and the side chain gives the comb polymer different structural characteristics and properties. Thus, the properties of the comb polymer, such as photoelectric property, hydrophilicity and lipophilicity and so on, can be adjusted by adjusting the structural compositions of the main chain and the length of the side chain.[25,26] Zheng *et al.*[27] have reported that the comb-like ionenes with aliphatic side chains were prepared and blended with a low density polyethylene (LDPE) for enhancing the antistatic and antimicrobial properties. Comb-like polymers have potential benefits over linear polymers due to having some special properties over other common polymers such as low tensile strength, low toxicity, biocompatibility, low density, low melting and boiling point and high solubility.[28] The structure of comb-like polymer, especially the varied packing manners of side chains, contributes the varied crystallization behavior.[29] The incorporating of side chains into the polymer main chain can suppress the crystallinity and enhance the solubility.[30]

In this study, the double comb-like quaternary ammonium salt polymers with the main chain containing quaternary ammonium salt groups are designed and synthesized, which have the advantages of good solubility in epoxy resin paints by increasing the branch length to reduce the polarity and crystallinity because of forming a double comb-shaped polymer structure. And the antistatic epoxy resin coatings are obtained by adding the double comb-like polymers as antistatic agents. The aim is to make the antistatic epoxy resin coatings reach the good antistatic performance with lower addition amount of double comb-like polymers. Thermal, electrostatic, morphological and physical properties of the antistatic epoxy resin coatings are valuated to verify the prepared double comb-like quaternary ammonium salt polymers to be the good antistatic agents.

2. Experimental

2.1. Materials

Epichlorohydrin, di-*n*-propylamine, di-*n*-butylamine, diethyl ether and silver nitrate were analytical grade and were purchased from Aladdin Co. Ltd. (China). Polyetheramine (D230) was purchased from Wuxi Xinmeng Electronic Material Co., Ltd. Epoxy resin (E-51) was purchased from Hangzhou Wuhuigang Adhesive Co., Ltd.

2.2 Synthesis of double comb-like quaternary ammonium salt polymers

2.2.1 Synthesis of P(DPA-EPI). Poly(di-*n*-propylamine-co-epichlorohydrin) [P(DPA-EPI)] was prepared by the polymerization reaction. The molar ratio of epichlorohydrin to di-*n*-propylamine was 1 : 1. Epichlorohydrin (EPI) was added dropwise with stirring to di-*n*-propylamine (DPA) in a round-bottomed flask at 0–10 °C. After the dropwise addition, the mixture was continually stirred for 2 h at 0–10 °C for addition reaction. Then the product was heated to 80 °C and reacted for 6 h to obtain the polymer. The polymer was cooled and extracted with diethyl ether to remove impurities. After dried in vacuum at 70 °C for 12 h, P(DPA-EPI) was obtained and stored in a dry closed container. The reaction equation is shown in Scheme 1.

2.2.2 Synthesis of P(DBA-EPI). Poly(di-*n*-butylamine-co-epichlorohydrin) [P(DBA-EPI)] was also prepared by the polymerization reaction using epichlorohydrin (EPI) and di-*n*-butylamine (DBA) as raw materials. The molar ratio of epichlorohydrin (EPI) to di-*n*-butylamine (DBA) was 1 : 1. The preparation process is the same as that of P(DPA-EPI). The reaction equation is shown in Scheme 1.

2.3 Antistatic epoxy resin coatings formulation and curing

The curable composition was prepared by mixing epoxy resin (E-51) and polyetheramine (D230) with the molar ratio of 2 : 1. Firstly, P(DPA-EPI) and P(DBA-EPI) were added to D230 with stirring to obtain a homogeneous solution, respectively. Then, E-51 was added in the solution with stirring. After stirring for two hour, the two kinds of antistatic epoxy resin paint were obtained. As a comparison, the epoxy resin paint was also prepared by mixing epoxy resin (E-51) and polyetheramine (D230) with the molar ratio of 2 : 1. The 150 μm thick layers of epoxy resin paint and the antistatic epoxy resin paints were applied on PP substrate using bar applicators. Then the paints were cured at 20 °C for 72 h to obtain the epoxy resin coating and antistatic epoxy resin coatings, respectively.

2.4 Characterization

Structure characterization of P(DPA-EPI) and P(DBA-EPI) were analyzed by X-ray powder diffraction (XRD, Bruker AXS D8 ADVANCE) and FT-IR spectrometer (VERTEX 80V, Brooke, German) in attenuated total reflection (ATR) mode. The final FT-IR spectrum of each sample was an average of 16 scans at a resolution of 4 cm^{-1} in the wavenumber range of 500–4000 cm^{-1}. Nuclear magnetic resonance spectra ^1H NMR ($CDCl_3$) were recorded on a BRUKER 600 MHz spectrometer at 298.15 K with 16 scans. The morphology of P(DPA-EPI) and P(DBA-EPI) were observed using transmission electron microscopy (TEM, JEM-2100 UHR). The decomposition behavior of P(DPA-EPI) and P(DBA-EPI) was detected by a TGA instrument (TG 209 F1, NETZSCH, German) from 35 to 400 °C at 10 °C min^{-1} in a nitrogen atmosphere.

2.5 Measurement of antistatic epoxy resin coatings

The morphology of the coatings was observed using the scanning electron microscopy (Hitachi, TM3000). In order to investigate the hydrophilicity of the antistatic epoxy resin coatings, the contact angles of the coatings were tested by an optical contact angle tester (DSA100, KRUSS Company, German) at 20 °C, relative humidity (RH) 60% and 15 μL of water drop. The thermal properties of epoxy resin coating and antistatic epoxy resin coatings were also tested by a TGA instrument (TG 209 F1, NETZSCH, German) from 50 to 800 °C at 10 °C min^{-1} in a nitrogen atmosphere. Surface resistivities (ρ_s) of the coatings were tested by the ultra-high resistance micro current meter (Shanghai Precision Scientific Instrument Co., Ltd., ZC-36) at 20 °C and relative humidity (RH) 60%. The hardness of the coatings was tested by a Rockwell hardness tester (HR-150A, Laizhou Huayu Zhongxin Testing Instrument Co., Ltd., China). The adhesion of the coatings was tested with Cross Cut Test and classified by ISO2409 standards (mtv Cross Cut Test CC 5000-1), which is the test method for assessing the resistance of coatings to separation from substrates when a right-

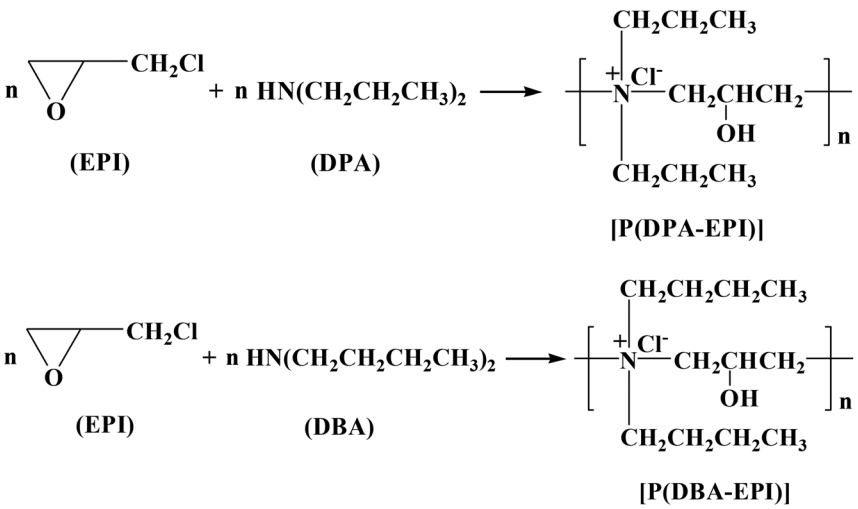

Scheme 1 The synthesis of P(DPA-EPI) and P(DBA-EPI).

angle lattice pattern is cut into the coating, penetrating through to the substrate.[31,32]

3. Results and discussion

3.1 Characterization of double comb-like quaternary ammonium salt polymers

3.1.1 Structure characterization. The XRD patterns of P(DPA-EPI) and P(DBA-EPI) are displayed in Fig. 1(a). The XRD patterns of P(DPA-EPI) and P(DBA-EPI) show broad weak peaks in the region $2\theta = 5$–$80°$, which might be due to the amorphous nature that does not exhibit any anisotropic behaviors.[30]

Fig. 1(b) shows the FT-IR spectra of EPI, DPA, DBA, P(DPA-EPI) and P(DBA-EPI). As shown in the FT-IR spectra of EPI, the absorption peaks at 1273 cm^{-1}, 964 cm^{-1} and 849 cm^{-1} belong to the C–O–C symmetric stretching vibration, C–O–C asymmetric stretching vibration and C–O–C skeleton stretching vibration,[33] respectively. As shown in the FT-IR spectra of DPA and DBA, the absorption peaks at 3460 cm^{-1} for DPA and at 3226 cm^{-1} for DBA belong to the –N–H stretching vibration.[34] As shown in the FT-IR spectra of P(DPA-EPI) and P(DBA-EPI), it can be seen that the C–O–C symmetric stretching vibration, C–O–C asymmetric stretching vibration, C–O–C skeleton stretching vibration and –N–H stretching vibration disappear. The O–H

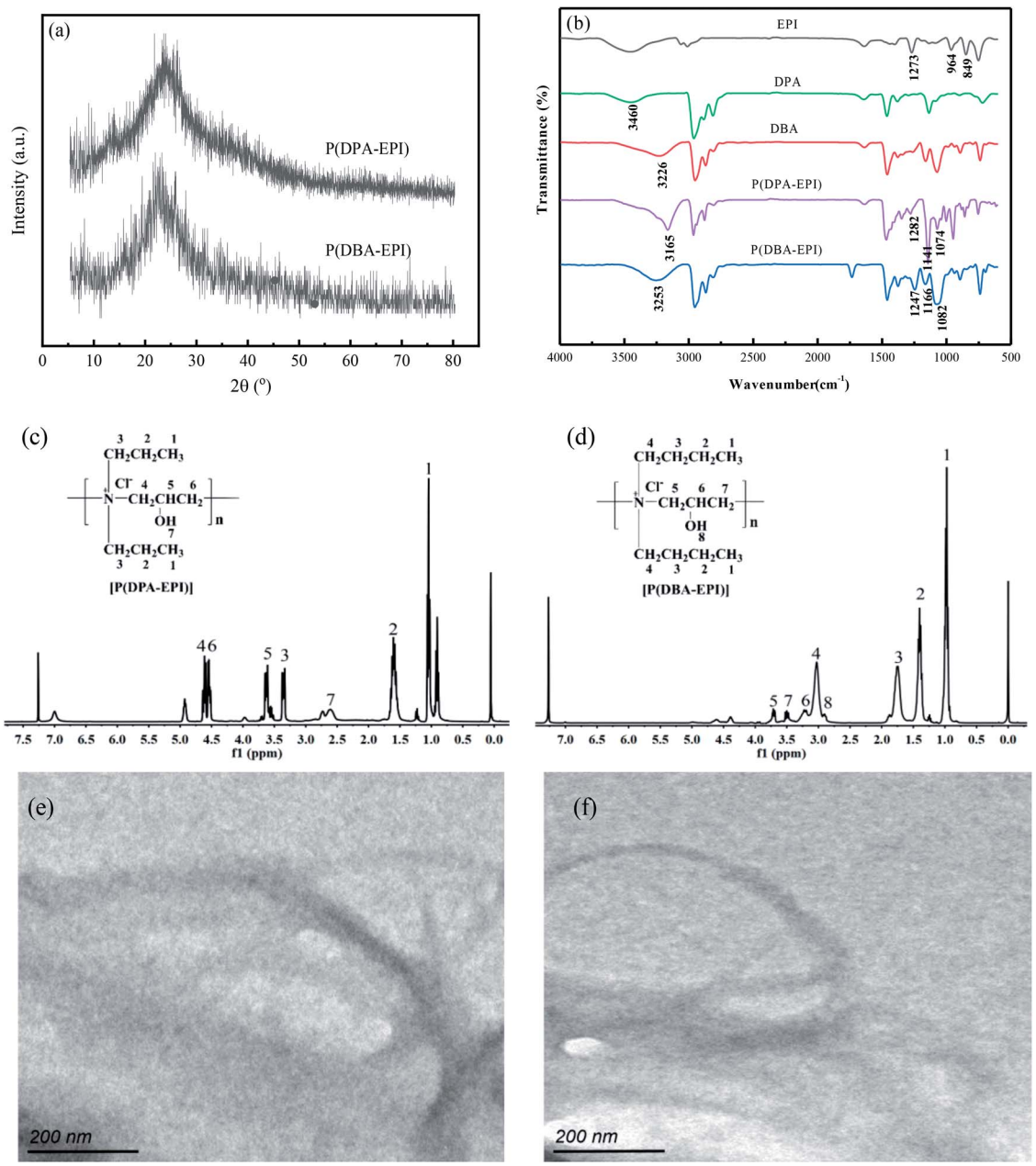

Fig. 1 (a) XRD spectra of P(DPA-EPI) and P(DBA-EPI), (b) FT-IR spectra of EPI, DPA, DBA, P(DPA-EPI) and P(DBA-EPI), ^{1}H NMR of (c) P(DPA-EPI) and (d) P(DBA-EPI) and TEM images of (e) P(DPA-EPI) and (f) P(DBA-EPI).

stretching vibration peaks[35] at 3165 cm^{-1} for P(DPA-EPI) and at 3253 cm^{-1} for P(DBA-EPI), the in-plane bending vibration peaks[36] at 1282 cm^{-1} for P(DPA-EPI) and at 1247 cm^{-1} for P(DBA-EPI) and the C–O stretching vibration peaks[37] at 1141 cm^{-1} for P(DPA-EPI) and at 1166 cm^{-1} for P(DBA-EPI) appear. All these imply that C–O–H bond is formed by epoxy groups opened and N–H bond broken. Meanwhile, the absorption peaks belonging to N–C_4 asymmetric stretching vibration at 1074 cm^{-1} for DPA[38] and at 1082 cm^{-1} for DBA[38] appear, indicating that the C–Cl bond is broken and C atom is bonded to the N atom of DPA and DBA to form an N–C bond, respectively. This can be confirmed by the experiment that the white precipitates of AgCl were formed when both the products of P(DPA-EPI) and P(DBA-EPI) were titrated with silver nitrate solution acidified by nitric acid because Cl^- is obtained by breaking the C–Cl bond. All these indicate that EPI reacts with DPA and DBA to generate P(DPA-EPI) and P(DBA-EPI), respectively.

The ^1H NMR ($CDCl_3$) spectra of P(DPA-EPI) and P(DBA-EPI) have been determined as shown in Fig. 1(c) and (d). From Fig. 1(c), the peaks at 0.97–1.10 ppm, 1.46–1.69 ppm, 3.30–4.40 ppm, 4.57–4.65 ppm, 3.58–3.68 ppm, 4.47–4.57 ppm and 2.50–2.78 ppm are assigned to 1-H, 2-H, 3-H, 4-H, 5-H, 6-H and 7-H, respectively. The result further speculates that P(DPA-EPI) was obtained. From Fig. 1(d), the peaks at 0.92–1.08 ppm, 1.32–1.53 ppm, 1.66–1.94 ppm, 2.97–3.18 ppm, 3.67–3.82 ppm, 3.18–3.34 ppm, 3.45–3.56 ppm and 2.87–2.97 ppm are assigned to 1-H, 2-H, 3-H, 4-H, 5-H, 6-H, 7-H and 8-H, respectively. The result further speculates that P(DBA-EPI) was obtained.

The representative TEM image of P(DPA-EPI) and P(DBA-EPI) presented in Fig. 1(e) and (f). Fig. 1(e) and (f) reveal the linear morphology of P(DPA-EPI) and P(DBA-EPI), respectively.

3.1.2 Thermogravimetric analysis. The thermal properties of P(DPA-EPI) and P(DBA-EPI) were determined using thermogravimetric curves. From Fig. 2, the TGA curves indicate that the weight loss before 100 °C is mainly due to the water adsorbed by P(DPA-EPI) and P(DBA-EPI). An initial thermal decomposition temperature is at 120 °C for both P(DPA-EPI) and P(DBA-EPI). And P(DPA-EPI) and P(DBA-EPI) present a sharp weight loss at 120–290 °C and 120–266 °C, respectively. Then they are basically decomposed completely. In short, P(DPA-EPI) and P(DBA-EPI) are relatively stable below 120 °C.

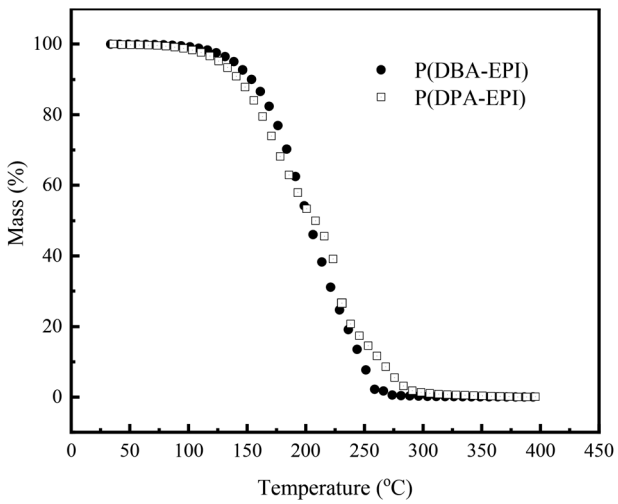

Fig. 2 The TGA curves of P(DPA-EPI) and P(DBA-EPI).

3.2 Surface morphology of antistatic epoxy resin coatings

To investigate the morphology of the antistatic epoxy resin sheets, the epoxy resin paint and antistatic epoxy resin paints were prepared using the method described in Section 2.3. Then pouring the epoxy resin paint and antistatic epoxy resin paints into the mold, 2 mm thick samples of epoxy resin sheet and the antistatic epoxy resin sheets were obtained after cured at 20 °C for 72 h and demolded at room temperature.

Fig. 3(a)–(c) are photographs of the epoxy resin sheet and the antistatic epoxy resin sheets (adding 1.0 wt% of P(DPA-EPI) and P(DBA-EPI), respectively) covering on the logo of Nanjing Forestry University. From Fig. 3(a)–(c), it can be seen that the three sheets are colorless and transparent. From Scheme 1, each nitrogen atom in the P(DPA-EPI) and P(DBA-EPI) molecule is connected with two propyl groups and two butyl groups, respectively. Introducing the propyl groups and butyl groups, the polarities of P(DPA-EPI) and P(DBA-EPI) molecules reduce. As a result, P(DPA-EPI) and P(DBA-EPI) have good solubility in epoxy resin paints, and the transparent antistatic epoxy resin sheets can be obtained.

SEM analysis of the epoxy resin coating and the antistatic epoxy resin coatings are presented in Fig. 3(d)–(i). It can be observed from Fig. 3(d) and (g) that the surface and cross section view of the epoxy resin coating is smooth, homogeneous, dense and defect-free. After adding 1.0 wt% of P(DPA-EPI) and P(DBA-EPI) in epoxy resin coating, respectively, the surface and cross section of obtained antistatic epoxy resin coatings are still smooth and homogeneous because of the good solubility and dispersion effect of P(DPA-EPI) and P(DBA-EPI) in epoxy resin paints, as shown in Fig. 3(e, f) and (h, i).

3.3 Electrostatic properties of antistatic epoxy resin coatings

3.3.1. Influence of addition amount of polymer. Fig. 4(a) shows the effect of addition amount of P(DPA-EPI) and P(DBA-EPI) on the surface resistivity (ρ_s) of antistatic epoxy resin coating at 20 °C and 60% of relative humidity (RH). The industry standards ANSI/EIA-541-1988 and ANSI/ESD S541-200 (USA) define the electrostatic dissipative material having the surface resistivity at 10^5–10^{12} and 10^4–10^{11} Ω sq^{-1},[28] respectively. When no double comb-like quaternary ammonium salt polymer is added, the value of ρ_s of the epoxy resin coating is 2.95×10^{12} Ω sq^{-1}, meaning that it is high in electric insulation. As shown in Fig. 4(a), the values of ρ_s of antistatic epoxy resin coating dramatically decrease with the addition of P(DPA-EPI) and P(DBA-EPI) until reach a threshold value (1.0 wt%). Beyond the threshold value, the values of ρ_s decrease slowly with further addition of P(DPA-EPI) and P(DBA-EPI), respectively.

The excellent antistatic properties of antistatic epoxy resin coatings can be explained by the compatibility of double comb-like quaternary ammonium salt polymers with epoxy resin

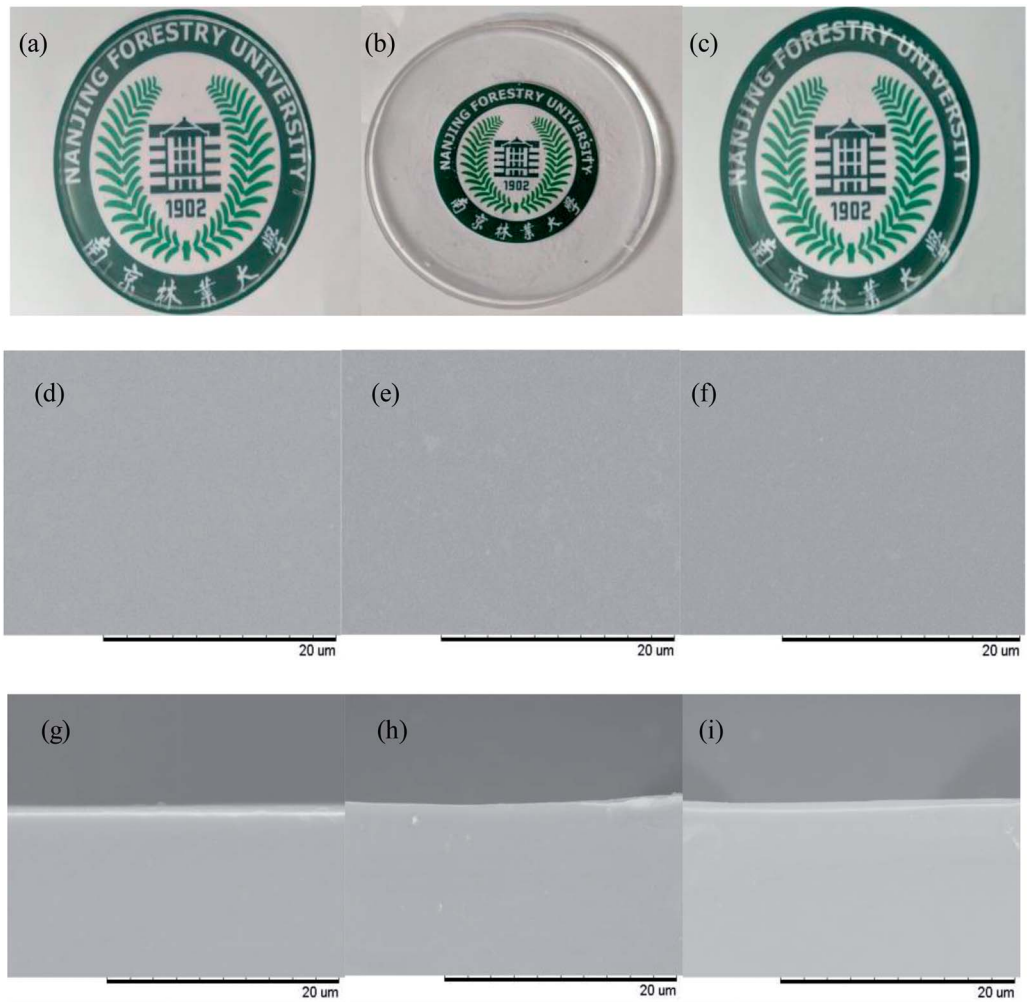

Fig. 3 (a–c) Photographs covering on the logo of Nanjing Forestry University, SEM images of (d–f) the surface and (g–i) the cross section of epoxy resin coating and the antistatic epoxy resin coatings. (a, d and g) Epoxy resin sheet and coatings, (b, e and h) antistatic epoxy resin sheet and coating adding 1.0 wt% of P(DPA-EPI), (c, f and i) antistatic epoxy resin sheet and coating adding 1.0 wt% of P(DBA-EPI).

coatings and the good hygroscopic performance of the polymers. The compatibility of double comb-like quaternary ammonium salt polymers with epoxy resin coatings can be confirmed from the SEM image. As shown in Fig. 3, the antistatic epoxy resin sheets are transparent and the surface and cross section of antistatic epoxy resin coatings are smooth and

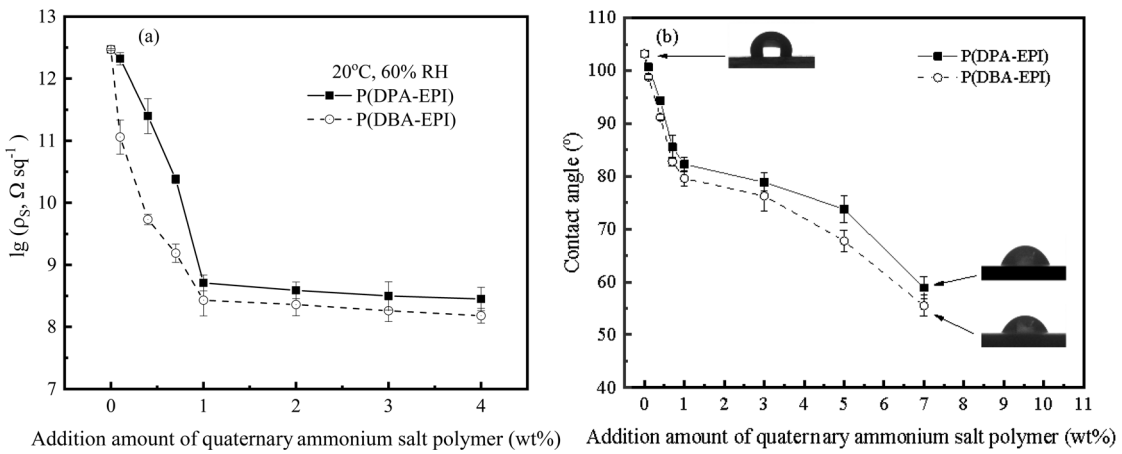

Fig. 4 (a) Surface resistivities (ρ_s) and (b) contact angles of antistatic epoxy resin coatings changes as the function of the addition amount of double comb-like quaternary ammonium salt polymer (wt%).

homogeneous meaning that P(DPA-EPI) and P(DBA-EPI) have good solution in epoxy resin paints and can be evenly dispersed in the coatings after being cured. In addition, Fig. 1(a) confirming a low degree of crystallinity of P(DPA-EPI) and P(DBA-EPI) means the solubility can be enhanced.[30]

The surface resistivity is related to the hygroscopic property of the coating. The increase of the polar groups, such as quaternary ammonium groups and hydroxyl groups in the coating, results in the increasing of the hygroscopic property of the coating, which conducts static electricity to make the surface resistivity reduce. As shown in Scheme 2, the water molecules can be adsorbed to form water film by the quaternary ammonium salts in evenly exposed P(DPA-EPI) and P(DBA-EPI) molecules on the surface of the coating, which leads to the reducing of surface resistivity by conducting static electricity. When the amount of the polymers is small, the polymer molecules are dispersed in epoxy resin coatings with isolation from each other, and the water adsorbed by the polymers cannot form a continuous water film. The values of surface resistivity are relatively high. With the increasing of the amount of the polymers, the P(DPA-EPI) and P(DBA-EPI) molecules are evenly dispersed in the epoxy resin coating to form a continuous molecular network structure because of the good compatibility between P(DPA-EPI) and P(DBA-EPI) molecules and epoxy resin coatings. The water adsorbed by the continuous polymer molecular network can form a continuous water film.[36] The static electricity can be conducted by the water film and the values of surface resistivity of the antistatic coatings decrease rapidly. When the continuous polymer molecular network structure tends to be complete with 1.0 wt% additive, the formed water film evenly covers all of coating surface, and most of the accumulated static electricity can be conducted out by the water film. Further increasing the amount of the polymers, the values of surface resistivity of the coatings decrease not obvious.

To confirm this finding, the surface analysis was performed by water contact angles. Fig. 4(b) displays the contact angles of the water droplets on the coatings determined as the function of double comb-like quaternary ammonium salt polymer concentration. From Fig. 4(b), the epoxy resin coating has a contact angle of 95° while this value decreases with the increasing of the amount of P(DPA-EPI) and P(DBA-EPI), respectively. The contact angles decline rapidly when the amount of P(DPA-EPI) and P(DBA-EPI) is lower than 1.0 wt%. Then the contact angles decline slowly with the further increasing of the amount of P(DPA-EPI) and P(DBA-EPI). The contact angle is related to the hygroscopic property of the coating. The introduction of P(DPA-EPI) and P(DBA-EPI) means increasing of the polar groups, such as quaternary ammonium salt and hydroxyl groups in the coating, which results in the increase of the polarity, hydrophilicity and wettability of the surface of the coating and the decrease of the contact angle. Therefore, the changes of water contact angle provide the evidence for the surface resistivity changes discussed above.

From Fig. 4(a), the values of ρ_s of the coatings reach 5.13×10^8 Ω sq^{-1} and 2.69×10^8 Ω sq^{-1}, respectively, with lower addition amount of P(DPA-EPI) and P(DBA-EPI) only 1.0 wt%. As shown in Scheme 1, both P(DPA-EPI) and P(DBA-EPI) molecules are double comb-like molecules. The main chains of P(DPA-EPI) and P(DBA-EPI) are all poly-quaternary ammonium salts composed of –N–$CH_2CH(OH)CH_2$– repeating units. And each N atom in the main chain of P(DPA-EPI) and P(DBA-EPI) links on two –$CH_2CH_2CH_3$ and –$CH_2CH_2CH_2CH_3$ side chains, respectively. It is difficult for the side chains to entangle each other because both –$CH_2CH_2CH_3$ and –$CH_2CH_2CH_2CH_3$ side chains are short chains. When the main chain is bent, the distance between the side chains on both sides of the main chain has changed. The distance on one side increases, while the distance on the other side decreases, showing that side chains have been compressed in this side. Due to the volume and exclusion effect in the compressed side, the molecular chain is not easy to crimp and entangle together, therefore, polymers P(DPA-EPI) and P(DBA-EPI) are easy to form linear morphology because molecular stretch arrangement is always energy wise favorable[28,39–41] as shown in Scheme 2. The morphology of P(DPA-EPI)

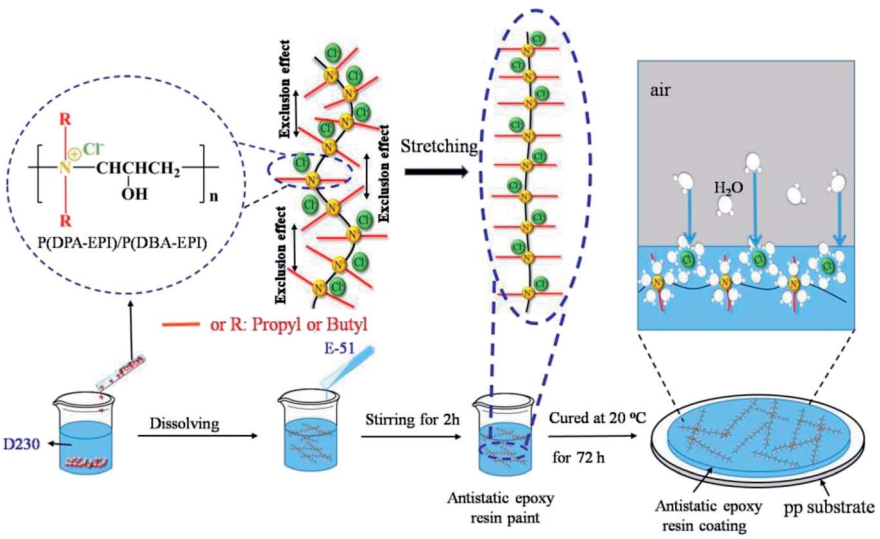

Scheme 2 Schematic representations of the antistatic mechanism.

and P(DBA-EPI) was further visualized by TEM images as shown in Fig. 1(e) and (f). The linear morphology makes the additive for overlapping to form a network structure reduce. Therefore, the antistatic epoxy resin coatings reach the good antistatic properties with lower addition amount of polymers only 1.0 wt%.

From Fig. 4(a), it also can be seen that the values of ρ_s of antistatic epoxy resin coating adding P(DBA-EPI) is less than that adding P(DPA-EPI), meaning that the hygroscopic performance of coating adding P(DBA-EPI) is greater than that adding P(DPA-EPI). As shown in Scheme 1, the main chain of P(DPA-EPI) has two $-CH_2CH_2CH_3$ side chains in each unit, while the main chain of P(DBA-EPI) has two $-CH_2CH_2CH_2CH_3$ side chains in each unit. So the distance between P(DBA-EPI) molecular chains is larger than that between P(DPA-EPI) molecular chains and the polarity of P(DBA-EPI) molecule is less than that of P(DPA-EPI) molecule, resulting P(DBA-EPI) is more soluble in epoxy resin paint than P(DPA-EPI). In addition, from Scheme 2, the graft chains of the double comb-like molecules have volume and exclusion effect. The increase in the length of the graft chains of the P(DBA-EPI) molecules causes the enhancement of the volume and exclusion effect. So the molecular chain of the P(DBA-EPI) is more difficult to crimp and entangle together compared to that of P(DPA-EPI), and the molecular chain arrangement of P(DBA-EPI) is closer to linear than that of P(DPA-EPI). As a result, the P(DBA-EPI) molecules can be more uniformly dispersed in the antistatic epoxy resin coating. Therefore, the water film on the surface of the coating formed by P(DBA-EPI) adsorbing moisture is denser, and the values of ρ_s of antistatic epoxy resin coating adding P(DBA-EPI) is less than that adding P(DPA-EPI). This can also be confirmed from the contact angle. The contact angles of the coating adding P(DBA-EPI) is less than that adding P(DPA-EPI) shown in Fig. 4(b).

3.3.2 Influence of relative humidity. Fig. 5 shows the influence of relative humidity (RH) on the surface resistivity (ρ_s) of antistatic epoxy resin coating at 20 °C. It can be seen from Fig. 5 that the relative humidity has a great influence on the surface resistivity. With the increasing of the relative humidity, the values of ρ_s decrease rapidly. This is for the reason that the P(DPA-EPI) and P(DBA-EPI) molecules on the surface of the coating can adsorb environment moisture resulting the reducing of the values of ρ_s. With the increasing of the relative humidity, the moisture adsorbed by the P(DPA-EPI) and P(DBA-EPI) molecules on the surface of the coating increases, therefore, the values of ρ_s rapidly decline. When the moisture adsorbed by the polymer molecules on the coating surface reaches equilibrium meaning the formed water film is relatively complete, the values of ρ_s do not decrease significantly with further increasing the relative humidity. So, when the value of relative humidity reaches 45%, the values of ρ_s decrease slightly with further increasing the relative humidity.

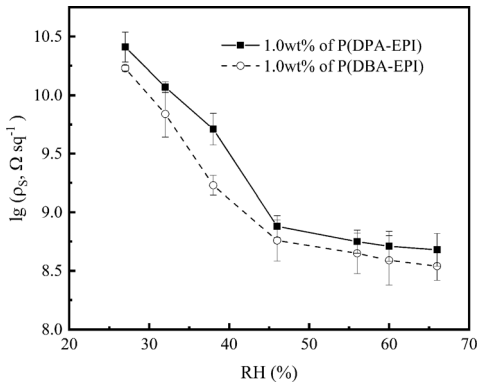

Fig. 5 Surface resistivity (ρ_s) of antistatic epoxy resin coating changing as a function of relative humidity at 20 °C.

3.4 Stability of antistatic epoxy resin coatings

3.4.1 Thermal stability. In order to compare the thermal properties of epoxy resin coating and antistatic epoxy resin coatings with adding 1.0 wt% of P(DPA-EPI) and P(DBA-EPI), respectively, they are prepared under the same conditions for TGA testing. TGA curves are shown in Fig. 6(a), and the inset figure is the partial enlarged curves. From Fig. 6(a), it can be seen that the onset decomposition temperature of the two antistatic epoxy resin coatings is about 364 °C, which is almost the same to that of the epoxy resin coating. When the temperature exceeds 364 °C, the weight loss curves of the antistatic epoxy resin coatings adding P(DBA-EPI) and P(DPA-EPI) are close to that of the epoxy resin coating, suggesting that the thermal stability of the antistatic epoxy resin coating is not obviously changed by the incorporation of P(DPA-EPI) and P(DBA-EPI).

The two antistatic epoxy resin coatings were heated for 24 h at different temperatures. After natural cooling to room temperature, the samples were exposed in air at 20 °C and 60% of relative humidity for 24 h, then the surface resistivities of the coatings were tested. As seen from Fig. 6(b), the heat treatment has a great influence on the surface resistivity. When the heat treatment temperature is lower than 120 °C, the values of ρ_s of the two antistatic epoxy resin coatings are almost unchanged. When the heat treatment temperature is higher than 120 °C, the values of ρ_s of the two antistatic epoxy resin coatings increase rapidly with the increasing of the heat treatment temperature. It is for the reason that P(DPA-EPI) and P(DBA-EPI) start to decompose as shown in the TGA curves (Fig. 2).

3.4.2 Washing durability. In order to compare the antistatic durability of the antistatic epoxy resin coating, two antistatic epoxy resin coatings with 1.0 wt% additive of P(DPA-EPI) and P(DBA-EPI) were selected for water washing experiment. The washing durability of antistatic epoxy resin coatings was tested as follows:[27] the antistatic epoxy resin coating was immersed into deionized water, taken out, and then scrubbed with adsorbent cotton, which was repeatedly performed for 50 times. The samples were exposed in air to be dried at 20 °C and 60% of relative humidity for 24–72 h, and then the values of ρ_s of the two coatings were measured. As shown in Fig. 7, the values of ρ_s of the two coatings after placed 24 h increase slightly than that before water washing, and the values after placed 72 h are close to that before water washing. This implies that the amount of loss of P(DPA-EPI) and P(DBA-EPI) from the coatings

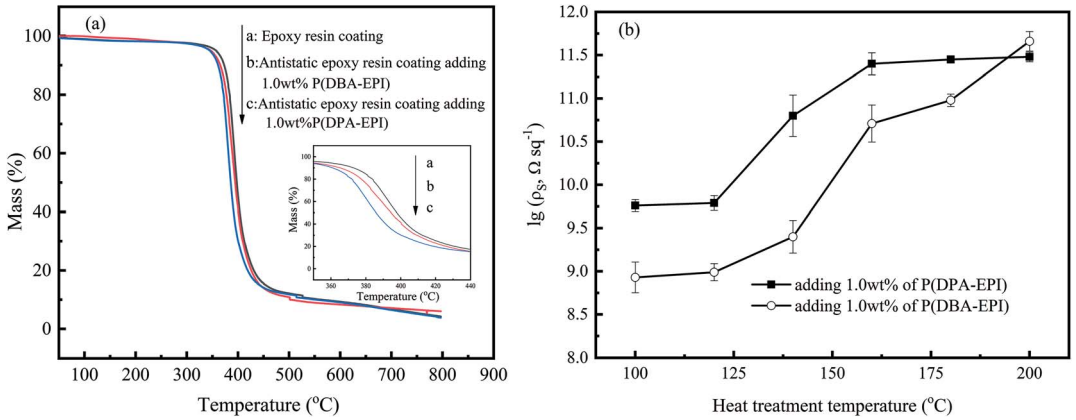

Fig. 6 (a) The TGA curve of epoxy resin coating and antistatic epoxy resin coatings (inset: an enlarged view of the curves) and (b) the thermal stability of antistatic epoxy resin coatings.

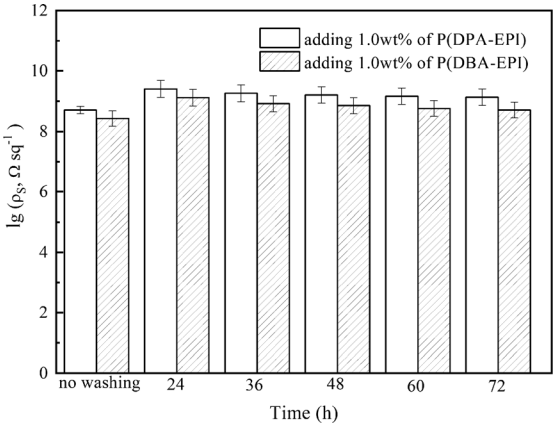

Fig. 7 The surface resistivity (ρ_s) tested after the coatings were washed with deionized water and placed at 20 °C and 60% of relative humidity for different times.

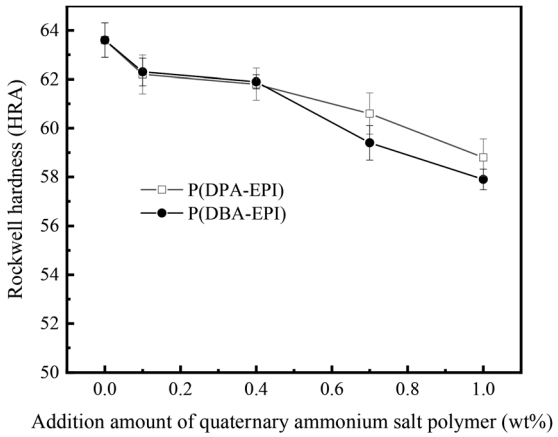

Fig. 8 Rockwell hardness of antistatic epoxy resin coatings and epoxy resin coating.

during washing is small, indicating that the two coatings have good antistatic properties and durability.

3.5 Physical properties of antistatic epoxy resin coatings

For engineering application of the coating material, hardness and adhesion are very important. The testing results of Rockwell hardness of antistatic epoxy resin coatings and epoxy resin coating are exhibited in Fig. 8. As illustrated in Fig. 8, the value of Rockwell hardness of epoxy resin coating is 63.2 HRA. The values of Rockwell hardness of antistatic epoxy resin coatings are lower than that of epoxy resin coating. This decrease in the Rockwell hardness values possibly results from the additive of P(DPA-EPI) and P(DBA-EPI) into the epoxy resin coating. P(DPA-EPI) and P(DBA-EPI) molecules dispersed in the epoxy resin coating increase the distance between the epoxy resin molecules, which makes the intermolecular force weaken, and the plasticity and flexibility of the coating increase. So the Rockwell hardness values of the antistatic epoxy resin coatings reduce.

The adhesion of the coatings was tested with Cross Cut Test and classified by ISO2409 standard. The testing results show that the edges of the two antistatic epoxy resin coatings and epoxy resin coating are smooth, the coatings do not detach, the classification was 0 according to the ISO 2490 standard, meaning that the edges of the incisions are perfectly smooth and the edges of the lattice are free of flaking. This indicates that the adhesion of epoxy resin coating does not obviously change with the introduction of P(DPA-EPI) and P(DBA-EPI).

4. Conclusions

In summary, two kinds of double comb-like quaternary ammonium salt polymer P(DPA-EPI) and P(DBA-EPI) were synthesized by the polymerization reaction. The transparent antistatic epoxy resin coatings were obtained using P(DPA-EPI) and P(DBA-EPI) as antistatic agents. The surface resistivity of the transparent antistatic epoxy resin coatings can be effectively reduced while basically maintained the original thermodynamic properties. Compared to the epoxy resin coating, the hardness values of the two antistatic epoxy resin coatings slightly reduce, and the adhesion of the two coatings do not

obviously change. These results demonstrate that the prepared P(DPA-EPI) and P(DBA-EPI) are promising candidate for antistatic agents for epoxy resin. The preparation of the double comb-like quaternary ammonium salt polymer, which is similar in polarity to the resin and can be dissolved in the resin, is an effective way to obtain an excellent antistatic agent.

Conflicts of interest

The authors declare that they have no known competing financial interests or personal relationships that could have appeared to influence the work reported in this paper.

Acknowledgements

This work was financially supported by the Natural Science Foundation of China (No. 50876047).

References

1 A. Jakubas and P. Jabłoński, *J. Electrost.*, 2015, **77**, 130–138.
2 X. Feng, J. Wang, C. Zhang, Z. Du, H. Li and W. Zou, *RSC Adv.*, 2018, **8**, 14740–14746.
3 W. Zieliński, K. A. Wilk, G. Para, E. Jarek, K. Ciszewski, J. Palus and P. Warszyński, *Colloids Surf., A*, 2015, **480**, 63–70.
4 H. He, Y. Yan, Z. Qiu and X. Tan, *Prog. Org. Coat.*, 2017, **113**, 110–116.
5 T. Iwata, A. Tsurumaki, S. Tajima and H. Ohno, *Polymer*, 2014, **55**, 2501–2504.
6 A. Tsurumaki, S. Tajima, T. Iwata, B. Scrosati and H. Ohno, *Electrochim. Acta*, 2017, **248**, 556–561.
7 S. M. M. Morsi, M. E. A. El-Aziz, R. M. M. Morsi and A. I. Hussain, *J. Coat. Technol. Res.*, 2019, **16**, 745–759.
8 J. Luo, X. Wang, J. Li, X. Zhao and F. Wang, *Polymer*, 2007, **48**, 4368–4374.
9 Y. Seki, M. Ince, N. Yıldız, Y. Seki, O. Ergül, K. Sever and M. Sarıkanat, *Polym.-Plast. Technol. Mater.*, 2019, **58**, 1471–1479.
10 M. Zhang, C. Zhang, Z. Du, H. Li and W. Zou, *Compos. Sci. Technol.*, 2017, **138**, 1–7.
11 Y. Tian, X. Zhang, H. Z. Geng, H. J. Yang, C. Li, S. X. Da, X. Lu, J. Wang and S. L. Jia, *RSC Adv.*, 2017, **7**, 53018–53024.
12 C. C. Hu, S. S. Chang and N. Y. Liang, *Text. Res. J.*, 2016, **86**, 1828–1836.
13 Y. Tao and D. C. Pan, *Mater. Res. Express*, 2019, **6**, 113563.
14 A. Mirmohseni, M. Rastgar and A. Olad, *J. Appl. Polym. Sci.*, 2020, **137**, 1–11.
15 W. Xiao, Y. Lei, Z. Xia, X. Chen, Y. Han and J. Nie, *J. Alloys Compd.*, 2017, **724**, 24–28.
16 Y. Cao, P. Xu, B. Wu, M. Hoch, P. J. Lemstra, W. Yang, W. Dong, M. Du, T. Liu and P. Ma, *Compos. Sci. Technol.*, 2020, **190**, 108043.
17 W. Zheng and S. C. Wong, *Compos. Sci. Technol.*, 2003, **63**, 225–235.
18 A. Tsurumaki, T. Iwata, M. Tokuda, H. Minami, M. A. Navarra and H. Ohno, *Electrochim. Acta*, 2019, **308**, 115–120.
19 Z. Yang, H. Peng, W. Wang and T. Liu, *J. Appl. Polym. Sci.*, 2010, **116**, 2658–2667.
20 L. Bao, J. Lei and J. Wang, *J. Electrost.*, 2013, **71**, 987–993.
21 Z. Yang, X. Liu, B. Gao, S. Zhao, Y. Wang, Q. Yue and Q. Li, *Sep. Purif. Technol.*, 2013, **118**, 583–590.
22 Y. L. Wang, Q. Bin Yan, Z. Guo, G. Guo, Q. Deng, J. Zhang and G. Chen, *Pet. Chem.*, 2018, **58**, 245–249.
23 L. Xing, L. Liu, F. Xie and Y. Huang, *Appl. Surf. Sci.*, 2016, **375**, 65–73.
24 X. Zhao, X. Wang, G. Song and T. Lou, *Int. J. Biol. Macromol.*, 2020, **156**, 585–590.
25 S. Houvenagel, L. Moine, G. Picheth, C. Dejean, A. Brûlet, A. Chennevière, V. Faugeras, N. Huang, O. Couture and N. Tsapis, *Biomacromolecules*, 2018, **19**, 3244–3256.
26 L. Chen, Z. Gu, L. Li, W. Lei, Q. Rong, C. Zhao, Q. Wu, Z. Gu, X. Jin, L. Jiang and M. Liu, *J. Mater. Chem. A*, 2018, **6**, 15147–15153.
27 A. Zheng, X. Xu, H. Xiao, Y. Guan, S. Li and D. Wei, *J. Mater. Sci.*, 2012, **47**, 7201–7209.
28 A. Sharma and P. P. Pande, *J. Polym. Mater.*, 2019, **36**, 175–194.
29 H. Mao, H. Wang, J. Li, L. Zhang, J. Shi and H. Shi, *Polymer*, 2020, **202**, 122721.
30 K. I. Aly, O. Younis, N. S. Al-Muaikel, A. A. Atalla, A. B. A. A. M. El-Adasy, M. A. Hussein and A. R. Abdellah, *J. Polym. Res.*, 2019, **26**, 1–13.
31 J. Do, D. Cha, I. Park, O. K. Kwon, J. Bae and J. Park, *Prog. Org. Coat.*, 2019, **128**, 59–68.
32 L. Kócs, M. H. Jilavi, M. Koch and P. W. de Oliveira, *Ceram. Int.*, 2020, **46**, 25865–25872.
33 X. Wang, N. Li, J. Wang, G. Li, L. Zong, C. Liu and X. Jian, *Compos. Sci. Technol.*, 2018, **155**, 11–21.
34 Y. Wu, F. Wang and Y. Huang, *Compos. Sci. Technol.*, 2018, **159**, 70–76.
35 H. Wang, R. Wang, R. Tao, Y. Zhu, C. Lv and Y. Zhu, *RSC Adv.*, 2016, **6**, 95556–95563.
36 A. Naderi, A. Dolati, A. Afshar and G. Palardy, *Mater. Chem. Phys.*, 2020, **244**, 122696.
37 M. A. Hussein, B. M. Abu-Zied and A. M. Asiri, *RSC Adv.*, 2018, **8**, 23555–23566.
38 W. Tian, Y. Hu, W. Wang and D. Yu, *RSC Adv.*, 2015, **5**, 91932–91936.
39 V. Danke, G. Gupta, S. Reimann, W. H. Binder and M. Beiner, *Eur. Polym. J.*, 2018, **103**, 116–123.
40 T. Babur, J. Balko, H. Budde and M. Beiner, *Polymer*, 2014, **55**, 6844–6852.
41 T. Babur, G. Gupta and M. Beiner, *Soft Matter*, 2016, **12**, 8093–8097.

